the FEBS Journal

Global shape and pH stability of ovorubin, an oligomeric protein from the eggs of *Pomacea canaliculata*

Marcos S. Dreon[1], Santiago Ituarte[1], Marcelo Ceolín[2] and Horacio Heras[1]

1 Instituto de Investigaciones Bioquímicas de La Plata (INIBIOLP), CONICET-UNLP, Argentina
2 Instituto de Investigaciones Físico-Químicas, Teóricas y Aplicadas (INIFTA), CONICET-UNLP, La Plata, Argentina and Universidad Nacional del Noroeste de Buenos Aires, Pergamino, Argentina

Keywords
carotenoprotein; mollusk; protease inhibitor; protein stability; protein structure

Correspondence
H. Heras, INIBIOLP – Fac. Cs. Médicas, 60 y 120, La Plata (1900), Argentina
Fax: +54 221 4258988
Tel: +54 221 4824894
E-mail: h-heras@atlas.med.unlp.edu.ar

(Received 16 May 2008, revised 3 July 2008, accepted 11 July 2008)

doi:10.1111/j.1742-4658.2008.06595.x

Ovorubin, a 300-kDa thermostable oligomer, is the major egg protein from the perivitellin fluid that surrounds the embryos of the apple snail *Pomacea canaliculata*. It plays essential roles in embryo development, including transport and protection of carotenoids, protease inhibition, photoprotection, storage, and nourishment. Here, we report ovorubin dimensions and global shape, and test the role of electrostatic interactions in conformational stability by analyzing the effects of pH, using small-angle X-ray scattering (SAXS), transmission electron microscopy, CD, and fluorescence and absorption spectroscopy. Analysis of SAXS data shows that ovorubin is an anisometric particle with a major axis of 130 Å and a minor one varying between 63 and 76 Å. The particle shape was not significantly affected by the absence of the cofactor astaxanthin. The 3D model presented here is the first for an invertebrate egg carotenoprotein. The quaternary structure is stable over a wide pH range (4.5–12.0). At a pH between 2.0 and 4.0, a reduction in the gyration radius and a loss of tertiary structure are observed, although astaxanthin binding is not affected and only minor alterations in secondary structure are observed. *In vitro* pepsin digestion indicates that ovorubin is resistant to this protease action. The high stability over a considerable pH range and against pepsin, together with the capacity to bear temperatures > 95 °C, reinforces the idea that ovorubin is tailored to withstand a wide variety of conditions in order to play its key role in embryo protection during development.

Pomacea canaliculata (Architaenioglossa: Ampullariidae) is a freshwater snail native to the Amazon and Plata basins, where its seasonal reproduction is mostly affected by changes in environmental temperatures and the availability of water [1–3]. During the 1980s, it was introduced into Asia, where it has both become a pest for rice crops and a vector for human eosinophilic meningoencephalitis, a parasitic disease that is rapidly expanding worldwide [4].

Most gastropod eggs have perivitellin fluid surrounding the fertilized oocyte that represents the major supply of nutrients during embryogenesis [5]. Ovorubin is the major protein in the perivitellin fluid of the eggs of *P. canaliculata*, previously described by Comfort [6] and Cheesman [7] as a carotenoprotein. It is a lipoglyco-carotenoprotein with a molecular mass of ~ 300 kDa, composed of three subunits of 28, 32 and 35 kDa [8], and it represents 60% of the total perivitellin fluid protein content [9]. The carotenoid content of ovorubin is mainly composed of astaxanthin (ASX), a potent membrane antioxidant [10] in its free and esterified forms. Ovorubin, besides its function as an energy and structural precursor donor, acts by transporting and stabilizing these labile antioxidants in the perivi-

Abbreviations
ASX, astaxanthin; R_g, gyration radius; SAXS, small-angle X-ray scattering; TEM, transmission electron microscopy.

tellin fluid [11]. In addition, Norden [12] has described this carotenoprotein as having trypsin, chymotrypsin and other protease inhibitor activity, another unusual function for a perivitellin.

In contrast to most invertebrate carotenoproteins, ovorubin does not suffer destabilization when its carotenoid is removed [11]. Moreover, the stabilities of apo-ovorubin and holo-ovorubin are virtually the same as regards structure stability against temperature; they remain stable over 95 °C and are affected only by molar concentrations of urea and guanidinium hydrochloride [13].

Except for the detailed studies on crustacyanin, the lobster carapace carotenoprotein, there is little information on the structure and stability of this interesting group of proteins, and there is no information in mollusks [14,15].

In this work, we report the first 3D low-resolution model of ovorubin obtained by small-angle X-ray scattering (SAXS). Ovorubin stability with regard to pH was also studied using SAXS, CD, intrinsic tryptophan fluorescence and absorption spectroscopy, in an attempt to further test its structural features.

Results

Global shape of ovorubin

Figure 1A shows the SAXS curves obtained for holo-ovorubin and apo-ovorubin normalized for protein concentration. Clearly, the two curves virtually overlap, indicating that both ovorubin forms have nearly the same shape and size. From the Guinier plot for holo-ovorubin and apo-ovorubin (Fig. 1A), it was possible to fit gyration radii of 43.0 ± 0.7 Å and 44.0 ± 0.1 Å, respectively. The Kratky plots (Fig. 1B) are bell-shaped, as expected for globular proteins. The gyration radii obtained are quite compatible with a compact oligomer of about 300 kDa, which is a molecular mass determined previously for ovorubin. Figure 1C shows the pair distribution curves obtained by means of the regularization technique implemented in GNOM4.5 [16]. Holo-ovorubin showed a maximum at 52 Å with a well-defined D_{max} of 122 Å, which is compatible with an anisometric particle. Apo-ovorubin showed a slightly displaced maximum and a higher contribution at longer distances, probably due to some degree of aggregation induced by the lack of the cofactor. A low-resolution model, obtained by averaging 16 calculated models using the algorithm implemented in DAMMIN [17], is depicted in Fig. 2A–C. This *ab initio* theoretical model fits satisfactorily with the experimental scattering intensity data (Fig. 2D). The particle

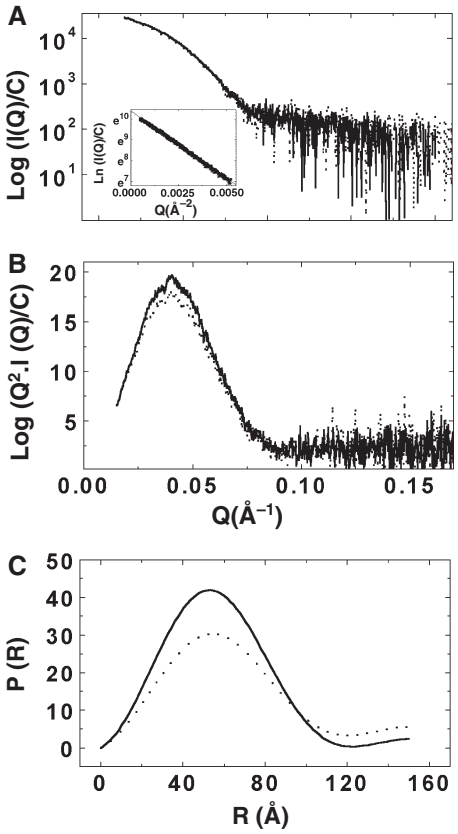

Fig. 1. Study of holo-ovorubin and apo-ovorubin solution structure by SAXS. (A) Raw SAXS data [$I(Q)$]. Inset: Guinier region in linearized variables. (B) Kratky plot [$I(Q)Q^2$] of data depicted in A. (C) Pair–distance distribution obtained from data in (A) using the program GNOM v4.5. Solid line: holo-ovorubin. Dotted line: apo-ovorubin.

shows an anisometric shape, with a major axis of 130 Å and a minor one varying between 63 and 76 Å.

Image analysis of transmission electron microscopy (TEM) data provided a size distribution curve of these particles showing a bimodal shape with two maxima, which account for more than 75% of the total (Fig. 3B). The diameter obtained from the first maximum, 112 Å, is in general agreement with the maximum pair distance obtained from SAXS results. The second maximum of the size distribution, 162 Å, is most likely an artefact resulting from sample processing. The absence of supramolecular aggregates observed by TEM is consistent with the SAXS results.

Structural stability of ovorubin with regard to pH

The gyration radius, R_g, of holo-ovorubin at different pH values is shown in Fig. 4A, where a constant value of 45 ± 2 Å can be observed between pH 12.0 and pH 4.5. The isoelectric point determined for holo-ovorubin was 4.9, and below this pH, a sudden

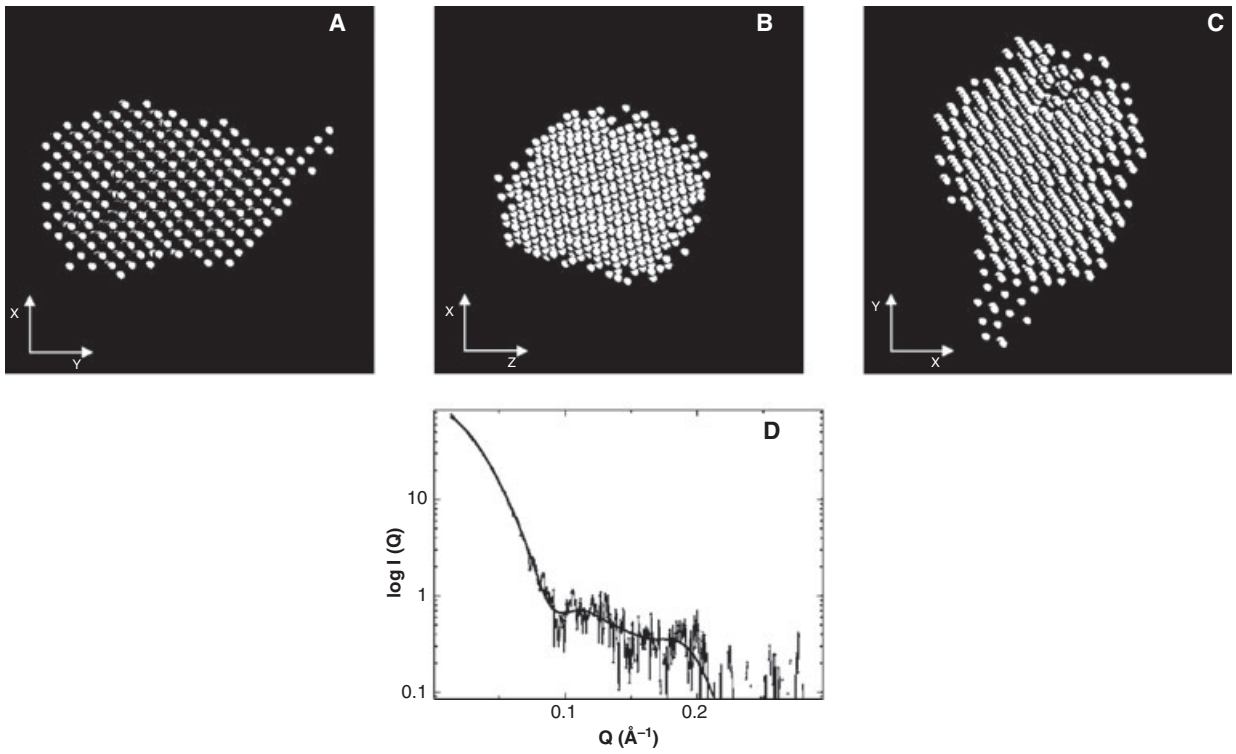

Fig. 2. Three-dimensional model of ovorubin from the eggs of *P. canaliculata*, obtained by analyzing the scattering data using the DAMMIN program in three different views. Referred to (A) view, (B) rotated 90° around *x*-axis, and (C) rotated 90° around *z*-axis. (D) Scattering intensity of experimental data for ovorubin (solid line) and theoretical *ab initio* dummy atom model (dotted line).

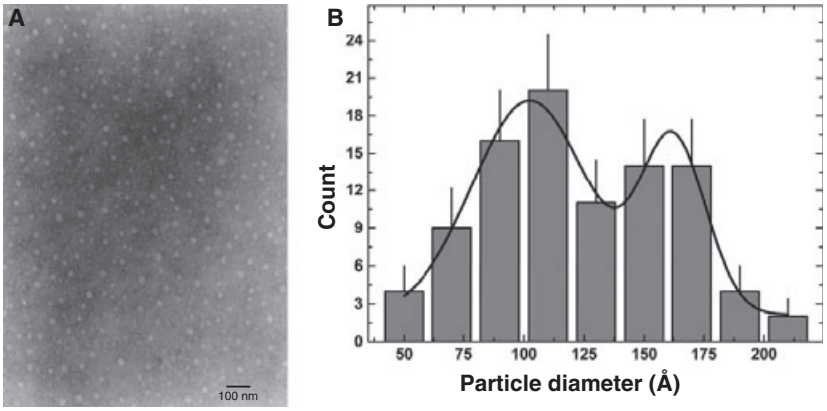

Fig. 3. Electron microscopy analysis of ovorubin from the eggs of the apple snail. (A) Electron micrograph of negatively stained ovorubin sample. Final magnification × 50 000. (B) Size distribution curve of ovorubin molecules. See Experimental procedures for details. Bar: 100 nm.

increase in R_g was observed before the onset of oligomer disassembly, observed from pH 4.0 to pH 2.0 as a constant decrease in the R_g value. The Kratky plots also showed a progressive loss of globularity at low pH values (Fig. 4B).

The absorption spectra of the protein at different pH values are displayed in Fig. 5. Only slight changes in the fine structure of the spectrum were observed at pH 2.0. Interestingly, neither red nor blue shifts were observed at all pH values assayed. It is known that the UV spectrum of ASX undergoes a large bathochromic shift, due to ASX binding to ovorubin, attributed to strong structural deformations of the carotenoid structure [18,19]. Lack of hypsochromism indicates that ASX remains bound to its binding site even under very acidic conditions.

The tryptophan fluorescence spectra between pH 2.0 and pH 12.0 (Fig. 6) show a red shift of its emission maxima (from 330 to 338 nm) and an intensity decrease at pH 2.0, indicative of the exposure of some of the tryptophan residues to the aqueous environment.

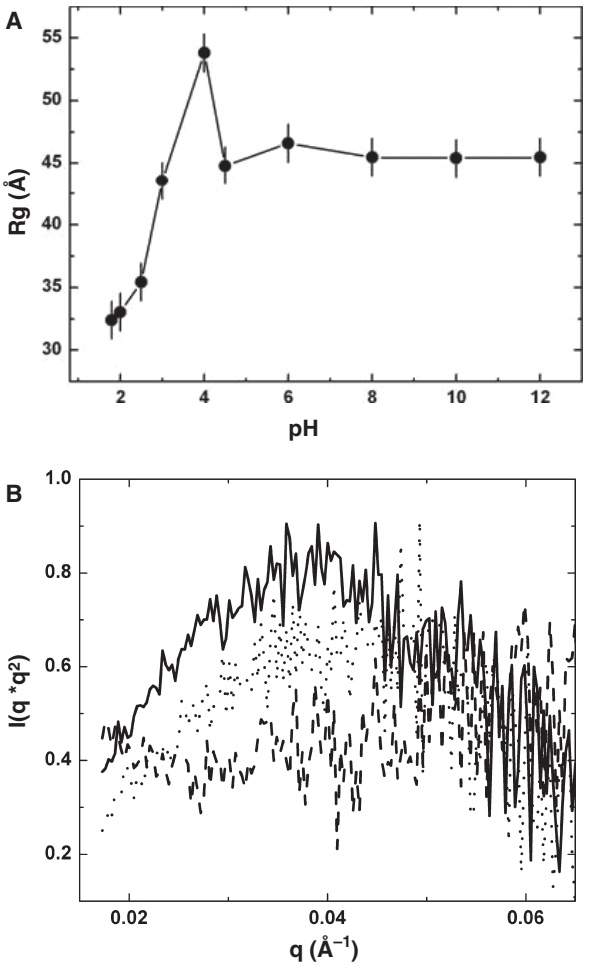

Fig. 4. Effect of pH on native ovorubin size and shape. (A) R_g of the particle as determined by SAXS. (B) Kratky plots for ovorubin at different pH values. Solid line: pH 6.0. Dotted line: pH 4.5. Dashed line: pH 2.0.

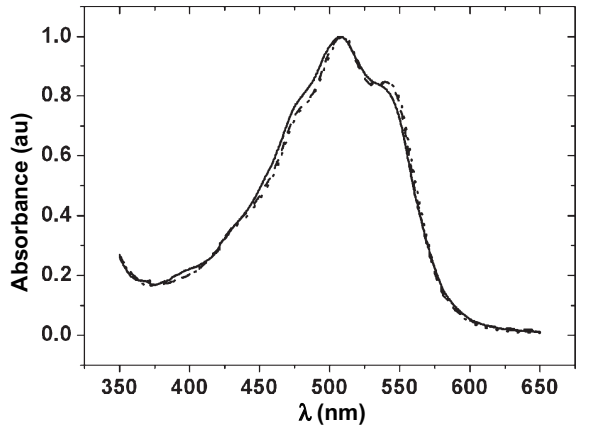

Fig. 5. Absorption spectra of ovorubin from *P. canaliculata* at different pH values. Solid line: pH 6.0. Dashed line: pH 2.0. Dotted line: pH 12.0.

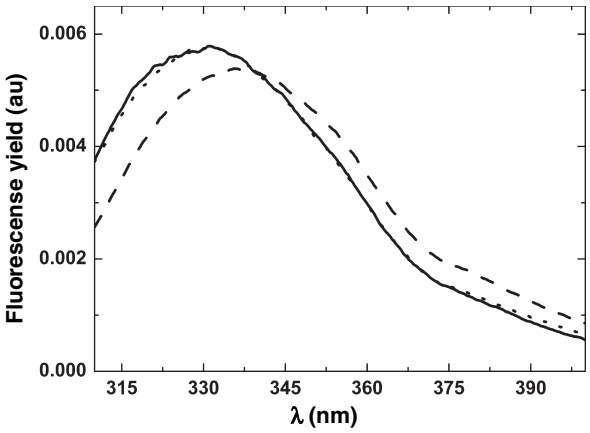

Fig. 6. Tryptophan fluorescence spectra of ovorubin at different pH values. Dashed line: pH 2.0. Solid line: pH 6.0. Dotted line: pH 12.0.

On the basis of the above results, the CD spectra in the near-UV and far-UV region were only recorded at pH 2.0 and pH 6.0 (Fig. 7). In the far-UV region (200–260 nm), both spectra were nearly coincident, indicating that the secondary structure of holo-ovorubin remains intact even at a low pH (Fig. 7A). Regarding the near-UV region (260–320 nm), a general loss of structure can be appreciated in the spectrum obtained at pH 2.0 in comparison with the one obtained at pH 6.0. No preferential loss of signal in the region of any of the aromatic residues was observed, suggesting a global loss of the tertiary structure of ovorubin.

Enzymatic digestion with pepsin was performed at acidic pH and at different preincubation times. It was observed that the oligomer was resistant to hydrolysis after a 150 min incubation, but degraded when preincubated for 48 h at pH 2.5 (Fig. 8).

Discussion

Size and solution structure of ovorubin

Ovorubin and crustacyanin are, so far, the only invertebrate carotenoproteins for which a 3D structure has been resolved, and a comprehensive body of information on the protein is available [11,13,19–24]. It is evident from these studies that the molluskan ovorubin complex differs in properties and molecular features from the crustacean carotenoprotein. Regarding the 3D structure, analysis of the SAXS scattering spectral data reveals that lobster crustacyanin has a cylindrical shape [21], whereas ovorubin is an anisometric protein. Another difference is the role that the carotenoid pigment ASX plays in the structural stability of these

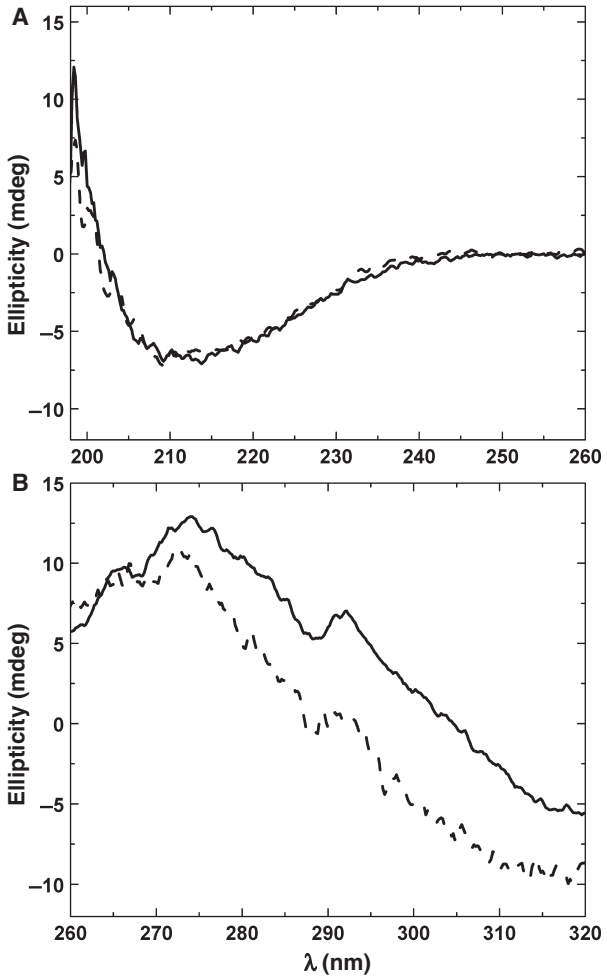

Fig. 7. CD spectra of ovorubin at different pH values. Spectra in the (A) near-UV region (260–320 nm) and (B) the far-UV region (200–260 nm). Solid line: pH 6.0. Dashed line: pH 2.0.

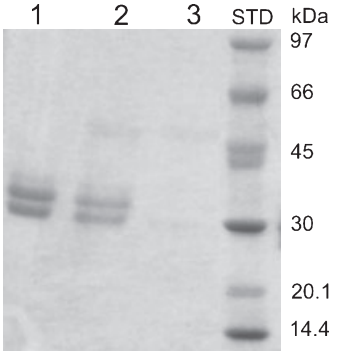

Fig. 8. Pepsin resistance of ovorubin analyzed on 4–20% SDS/PAGE. Lane 1: negative control ovorubin incubated for 150 min at pH 2.5 (6 μg). Lane 2: pepsin-digested ovorubin (6 μg). Lane 3: ovorubin (6 μg) preincubated for 48 h at pH 2.5 and then digested with pepsin. Lane 4: molecular mass markers.

proteins: ASX is essential for crustacyanin integrity [21], which contrasts with the situation for ovorubin, where it plays virtually no role in the stability of the oligomer [11,13], thus indicating a very different interaction between subunits in the two carotenoproteins. Using the *ab initio* program DAMMIN, we have modeled the shape of ovorubin as a compact complex of 130×76 Å. Negatively stained purified ovorubin appeared in electron micrographs also as anisometric particles with a maximum size of 112 Å (assuming that the larger particles are experimental artefacts). This is convergent with the SAXS data regarding global shape and dimensions, and differs from data on other invertebrate carotenoproteins such as the lobster crustacyanin (a cylinder of 238×95 Å) [21] and the starfish linckiacyanin (a spring-like structure with a diameter of 200–260 Å) [25], which have functions quite different from the role of ovorubin in the eggs of apple snails (Table 1).

Physiological and biophysical implications of stability with regard to pH

Overall, carotenoproteins belong to a group of proteins that are stable over a relatively wide pH range [26]. Although this fact has not been previously studied in the phylum Mollusca, there are several examples in crustaceans and echinoderms (Table 1).

Ovorubin, the first molluskan carotenoprotein so far studied shows structural stability over a wider pH range than that of the crustaceans or echinoderm proteins. Remarkably, ovorubin is the only carotenoprotein stable at pH 12. At this pH, the lysyl and arginyl residues are neutralized, usually affecting the quaternary structure. The high stability of ovorubin oligomers might be due to a shift of the pK of the amino acid residues beyond 12, owing to their involvement in salt bridges. At acidic pH, the stability of ovorubin was similar to that of all other carotenoproteins (Table 1).

As mentioned above, electrostatic forces are crucial for stabilization of the ovorubin quaternary structure, as suggested by the strong decrease in the R_g at pH values below 4.0.

The sharp increase in R_g obsrved at pH 4.5 is probably due to partial unfolding of the subunits, leading to their dissociation. In addition, the isoelectric point determined at pH 4.9 suggests that alterations in the charge of the molecule are taking part in the R_g change. All these results indicate that, around this pH, the native structure of ovorubin becomes unstable, leading to the disassembly observed at a lower pH.

Table 1. Stability with regard to pH of aquatic invertebrate carotenoproteins.

Taxa	Species	Carotenoprotein/location	pH range	Ref.
Arthropoda: Crustacea	*Procambarus clarkii*	Blue/carapace	5.5–8.0	[26]
Arthropoda: Crustacea	*Upogebia pusilla*	Blue/carapace	5.5–9.0	[41]
Arthropoda: Crustacea	*Homarus americanus*	Crustacyanin/carapace	5.0–8.5	[42]
Echinodermata: Asteroidea	*Marthasterias glacialis*	Blue/skin	4.0–8.5	[43]
Echinodermata: Asteroidea	*Marthasterias glacialis*	Purple/skin	3.5–8.5	[43]
Arthropoda: Crustacea	*Homarus americanus*	Ovoverdin/egg	4.0–9.0	[44]
Mollusca: Gastropoda	*Pomacea canaliculata*	Ovorubin/egg	4.0–12.0	Present paper

The lack of differences in the absorption spectra of ovorubin in the pH range assayed clearly indicate that residues in the ASX-binding site were not charged, suggesting that the residues involved in ASX binding, responsible for the bathochromic effect, are not ionizable polar residues. This is in agreement with previous studies of tryptophan resonance energy transfer to ASX, which indicate that the carotenoid-binding site is a nonpolar environment [13].

In other words, at pH 2.0 there is a decrease in R_g, indicative of disassembly of the particle, but there are no changes in the absorption spectrum of ovorubin, indicating that ASX is not located in the subunit interface involved in the stabilization of the oligomer. This is in agreement with previous reports on the stability of apo-ovorubin and holo-ovorubin against temperature and chaotropes [13]. Other serine protease inhibitors have a similarly high stability, ranging from pH 2 to pH 12 [27]. It must be remarked that the major loss of tertiary and quaternary structure was not enough to promote the detachment of the ASX molecule from ovorubin, indicating that the structure of the carotenoid-binding site is mainly dominated by secondary structure elements. Moreover, an indirect indication that ovorubin is susceptible to hydrolysis at acidic pH came from the pepsin digestion experiment. When ovorubin was preincubated for 48 h at pH 2.5, it lost its resistance towards the enzyme that was observed at short incubation times.

Eggs of *P. canaliculata* have a conspicuous warning coloration that signals to potential predators the presence of unpalatable or toxic compounds [28]. Snail eggs were therefore thought to be unpalatable [29], and in fact have a small number of predators. The pH stability of ovorubin is within the pH range of vertebrate digestive tract fluids [30,31], and the present results indicate that the protein can withstand the combined effect of low pH values and enzymatic attack for more than 2 h. Thus, if the eggs are ingested by a predator, ovorubin could reach the intestine in a fully active form and exert its potent trypsin inhibitor action, formerly thought to be only antimicrobial [12]. It could therefore be speculated that ovorubin is actively involved in the chemical defense of the embryos by limiting the predator's ability to digest and use essential nutrients from the eggs, thus rendering the ingestion of *P. canaliculata* eggs antinutritive.

The ovorubin complex, despite its large size and oligomeric nature, now appears to be a protein tailored to withstand a variety of extreme conditions, reinforcing the idea it plays a key role in embryo development.

Ongoing research is looking further into the antitrypsin properties of the molecule.

Experimental procedures

Egg collection

Adults of *P. canaliculata* were collected in streams or ponds near La Plata, a province of Buenos Aires, Argentina. Eggs were collected from females either raised in our laboratory or taken from the wild between November and April (reproductive season). Embryo development was checked in each egg mass microscopically [8], and only egg masses having embryos developed to no more than the morula stage were used.

Ovorubin isolation and purification

Fertilized eggs were repeatedly rinsed with ice-cold 20 mM Tris/HCl (pH 6.8), containing 0.8 μM aprotinin (Trasylol, Mobay Chemical Co., New York, Ny, USA) and homogenized in a Potter-type homogenizer (Thomas Sci., Swedesvoro, NJ, USA) in the dark and under an N_2 atmosphere. The buffer/sample ratio was kept at 5 : 1 v/w [32]. The crude homogenates were then sonicated for 15 s and centrifuged at 10 000 ***g*** for 30 min, and then at 100 000 ***g*** for 60 min. The pellet was discarded, and the supernatant was stored at −70 °C until analysis. Protein content was determined by the method of Bradford *et al.* [33], using BSA as standard.

The soluble protein fraction obtained using the above procedure was purified in a Merck-Hitachi high-performance liquid chromatograph (Hitachi Ltd, Tokyo, Japan)

with an L-6200 Intelligent Pump and an L-4200 UV detector set at 280 nm. A serial HPLC purification was performed. First, the sample was analyzed in a Mono Q HR 10/10 (Amersham-Pharmacia, Uppsala, Sweden), using a gradient of 0–1 M NaCl in 20 mM Tris buffer. The ovorubin peak was then further purified by size exclusion chromatography (Superdex 200 HR 10/20; Amersham-Pharmacia, Uppsala, Sweden), using an isocratic gradient of 50 mM sodium phosphate buffer and 150 mM NaCl (pH 7.6). The purity of the single peak obtained was checked by native electrophoresis.

A solution of 2 $mg{\cdot}mL^{-1}$ apo-ovorubin was prepared as previously described [13].

Gel electrophoresis

Nondissociating electrophoresis was performed on a 4–20% polyacrylamide gradient [34,35]. The gels were stained with Coomassie Brilliant Blue R-250 (Sigma Chemical Co, St Louis, MO, USA).

SAXS

SAXS experiments were performed either at the D11A-SAXS1 or the D02A-SAXS2 lines operating in the Laboratorio Nacional de Luz Syncrotron, Campinas (SP, Brazil). The scattering pattern was detected either using a gas-filled one-dimensional position-sensitive detector with an active window of 80 mm (SAXS1) or a MARCCD bidimensional charge-coupled device assisted by FIT 2D software (http://www.esrf.fr/computing/scientific/FIT2D) (SAXS2). The experiments were performed using a wavelength of 1.448 Å for the incident X-ray beam to minimize carbon absorption. The distance between the sample and the detector was kept at 1044 mm, allowing a Q-range between 0.012 and 0.25 $Å^{-1}$ ($D_{max} \leq 260$ Å). The temperature was controlled using a circulating water bath, and kept at 15 °C. Each individual run was corrected for sample absorption, photon flux, buffer scattering, and detector homogeneity. At least three independent curves were averaged for each single experiment. SAXS experiments in a protein range of 2.4–0.20 $mg{\cdot}mL^{-1}$ were performed to rule out a concentration effect in the data. The final experiments were performed at 0.24 $mg{\cdot}mL^{-1}$. The distance distribution function $P(r)$ was calculated by the Fourier inversion of the scattering intensity $I(q)$ using the GNOM 4.5 program [16]. The low-resolution model of ovorubin was obtained from the algorithm built in the program DAMMIN [36]. The program DAMMIN uses simulated annealing optimization to generate a bead model giving the best fit to the scattering intensity. The resulting dummy atom model represents the shape of the scattering particle. To increase the reliability of the results, the final model for the dummy atom modeling was obtained by a spatial average of 16 independent low-resolution models, calculated with the package program DAMAVER [37].

TEM

Samples for TEM of native ovorubin of 3 $mg{\cdot}mL^{-1}$ in 20 mM phosphate buffer (pH 7.4) were stained with 1% (w/v) sodium phosphotungstate (pH 7.4), blotted and air-dried. Images were recorded under low-dose conditions in a JEM-1200 EX transmission electron microscope (Tokyo, Japan). Statistical analysis of the particle size distribution was carried out using the tools built into the program IMAGEJ 1.36b (http://rsb.info.nih.gov/ij/).

Ovorubin stability with regard to pH

In order to evaluate the influence of pH on ovorubin structure, solutions of 0.24 $mg{\cdot}mL^{-1}$ of the protein at different pH values (from 2 to 12) were prepared using sodium phosphate salts and citric acid. All buffers employed were 0.1 M sodium phosphate salts, except for the pH 4 buffer, which was prepared by mixing 0.1 M sodium citrate and 0.2 M Na_2HPO_4 [38].

After 48 h of incubation, samples were analyzed by SAXS, CD, and fluorescence and absorption spectroscopy.

Ovorubin isoelectric point determination by 2D electrophoresis

Immobiline DryStrips (7 cm; pH 4–7, GE Healthcare, Uppsala, Sweden) were rehydrated overnight with rehydration buffer (0.5% immobilized pH gradient buffer 4–7 in Milli-Q water, and traces of bromophenol blue) containing approximately 0.5 μg of purified ovorubin. Running was performed in an Ettan IPGphor 3 IEF system from GE Healthcare. Electrical conditions were as described by the supplier. After the first-dimension run, the immobilized pH gradient gel strips were incubated at room temperature in 3 mL of equilibration buffer (50 mM Tris, pH 6.8, and traces of bromophenol blue) prior to separation in the second dimension. The second-dimension PAGE electrophoresis was performed in a vertical system with uniform 10% separating gel, at 25 °C. The ovorubin spot in the 2D gel was visualized by Coomassie Brilliant Blue R-250 stain (Sigma Chemicals).

Pepsin resistance

To analyze pepsin resistance, 20 μg of ovorubin was incubated for 150 min in 0.02 mL of 150 mM NaCl (pH 2.5), adjusted with 1 M HCl in the presence or absence of 1 μg of pepsin (Sigma; product No. P6887) [39]. Assays were performed with preincubation of ovorubin at pH 2.5 for 48 h before pepsin was added. The proteins were analyzed by 4–20% SDS/PAGE.

CD and visible absorption spectroscopy measurements

CD spectra were made either in a Jasco Inc. J-720 spectropolarimeter or in a J-810 spectropolarimeter (USA), using 0.2 mm cells placed in a thermostated cell holder at 15 °C. Samples were measured at a concentration of 0.06 mg·mL^{-1} in 0.1 M phosphate buffer at pH 6 and pH 2. Scanning was performed with a 1 nm bandwidth, a 100-nm·min^{-1} scan speed, and a 4s average time. Each spectrum was obtained by averaging at least five individual runs, and corrected for buffer optical activity. Secondary structure content was estimated by analysis of the molar ellipticities with the K2D algorithm [40].

Fluorescence and absorption spectroscopy measurements

Tryptophan fluorescence spectra of ovorubin at pH 2, pH 6 and pH 12 in 0.1 M phosphate buffer were recorded in emission scanning mode (SLM Aminco, Urbana, IL, USA). Tryptophan emission was excited at 290 nm (5 nm slit) and recorded between 310 and 410 nm (5 nm slit). The measurements were made in 5 mm optical path length quartz cells placed in a thermostated cell holder kept at 20 °C. Each spectrum was corrected for buffer fluorescence and averaged from at least two independent runs. Similarly, absorption spectra (350–650 nm) for each pH value were taken.

Acknowledgements

This work was partially supported by CONICET PIP No. 5888. M. S. Dreon is a member of Carrera del Investigador CICBA, Argentina. H. Heras and M. Ceolín are members of Carrera del Investigador CONICET, Argentina. S. Ituarte is a doctoral fellow of CONICET, Argentina. We also thank LNLS – Brazilian Synchrotron Light Laboratory/MCT for access to their facilities and partial financial support (Projects D11A-SAXS1-5207/06 and 5267).

We thank Dr M. Ermácora for kindly providing access to the CD equipment.

References

1 Albrecht EA, Carreño NB & Castro-Vazquez A (1999) A quantitative study of environmental factors influencing the seasonal onset of reproductive behaviour in the south American apple-snail *Pomacea canaliculata* (Gastropoda: Ampullariidae). *J Molluscan Stud* **65**, 241–250.

2 Pizani NV, Estebenet AL & Martin PR (2005) Effects of submersion and aerial exposure on clutches and hatchlings of *Pomacea canaliculata* (Gastropoda: Ampullariidae). *Am Malacol Bull* **20**, 55–63.

3 Albrecht EA, Koch E, Carreño NB & Castro-Vazquez A (2005) Control of the seasonal arrest of copulation and spawning in the apple snail *Pomacea canaliculata* (Prosobranchia: Ampullariidae): differential effects of food availability, water temperature, and day length. *Veliger* **47**, 169–174.

4 Cowie RH (2002) Apple snails as agricultural pests: their biology, impacts, and management. In *Molluscs as Crop Pests* (Baker GM, ed), pp. 145–192. CABI, Wallingford.

5 de Jong-Brink M, Boer HH & Joosse J (1983) Mollusca. In *Reproductive Biology of Invertebrates. Oogenesis Oviposition and Oosorption* (Adiyodi KG & Adiyodi RG, eds), pp. 297–355. Wiley, New York, NY.

6 Comfort A (1947) Lipochromes in the ova of *Pila*. *Nature* **160**, 333–334.

7 Cheesman DF (1958) Ovorubin, a chromoprotein from the eggs of the gastropod mollusk *Pomacea canaliculata*. *Proc R Soc Lond [Biol]* **149**, 571–587.

8 Garín CF, Heras H & Pollero RJ (1996) Lipoprotein of the egg perivitellin fluid of *Pomacea canaliculata* snails (Mollusca: Gastropoda). *J Exp Zool* **276**, 307–314.

9 Dreon MS, Heras H & Pollero RJ (2003) Metabolism of ovorubin, the major egg lipoprotein from the apple snail. *Mol Cell Biochem* **243**, 9–14.

10 Palozza P & Krinsky NI (1992) Astaxanthin and cantaxanthin are potent antioxidants in a membrane model. *Arch Biochem Biophys* **297**, 291–295.

11 Dreon MS, Schinella G, Heras H & Pollero RJ (2004) Antioxidant defense system in the apple snail eggs, the role of ovorubin. *Arch Biochem Biophys* **422**, 1–8.

12 Norden DA (1972) The inhibition of trypsin and some other proteases by ovorubin, a protein from the eggs of *Pomacea canaliculata*. *Comp Biochem Physiol* **42**, 569–576.

13 Dreon MS, Ceolín M & Heras H (2007) Astaxanthin binding and structural stability of the apple snail carotenoprotein ovorubin. *Arch Biochem Biophys* **460**, 107–112.

14 Zagalsky PF, Wright CE & Parsons M (1995) Crystallisation of alpha-crustacyanin, the lobster carapace astaxanthin-protein: results from EURECA. *Adv Space Res* **16**, 91–94.

15 Zagalsky PF, Clark RJH & Fairclough DP (1983) Resonance Raman and circular dichroism studies of the copepod (*Anomalocera patersoni*) and siphonophore (*Porpita* sp.) astaxanthin-proteins with an identical absorption maximum at 650 nm. *Comp Biochem Physiol* **75**, 169–170.

16 Svergun DI (1992) GNOM 4.5. *J Appl Crystallogr* **25**, 495–503.

17 Svergun DI, Petoukhov MV & Koch MHJ (2001) Determination of domain structure of proteins from x-ray solution scattering. *Biophys J* **80**, 2946–2953.

18 Clark RJH, D'Urso NR & Zagalsky PF (1980) Exitation profiles, absorption and resonance Raman spectra of the carotenoprotein ovorubin, and a resonance Raman study of some other astaxanthin proteins. *J Am Chem Soc* **102**, 6693–6698.
19 Zagalsky PF, Eliopoulos EE & Findlay JB (1990) The architecture of invertebrate carotenoproteins. *Comp Biochem Physiol* **97**, 1–18.
20 Chayen NE, Cianci M, Olczak A, Raftery J, Rizkallah PJ, Zagalsky PF & Helliwell JR (2000) Apocrustacyanin A1 from the lobster carotenoprotein alpha-crustacyanin: crystallization and initial X-ray analysis involving softer X-rays. *Acta Crystallogr* **56**, 1064–1066.
21 Dellisanti CD, Spinelli S, Cambillau C, Findlay JBC, Zagalsky PF, Finet S & Receveur-Brechot V (2003) Quaternary structure of alpha-crustacyanin from lobster as seen by small-angle X-ray scattering. *FEBS Lett* **544**, 189–193.
22 Dreon MS, Heras H & Pollero RJ (2004) Characterization of the major egg glycolipoproteins from the perivitellin fluid of the apple snail *Pomacea canaliculata*. *Mol Reprod Dev* **68**, 359–364.
23 Heras H, Dreon MS, Ituarte S & Pollero RJ (2007) Egg carotenoproteins in neotropical Ampullariidae (Gastropoda: Arquitaenioglossa). *Comp Biochem Physiol* **146**, 158–167.
24 Zagalsky PF, Mummery RS, Eliopoulos EE & Findlay JBC (1990) The quaternary structure of the lobster carapace carotenoprotein, crustacyanin: studies using cross-linking agents. *Comp Biochem Physiol* **97**, 837–848.
25 Zagalsky PF, Haxo F, Hertzberg S, Hertzberg S & Liaaen-Jensen S (1989) Studies on a blue carotenoprotein, linckiacyanin, isolated from the starfish *Linckia laevigata* (Echinodermata: Asteroidea). *Comp Biochem Physiol* **93**, 339–353.
26 Garate AM, Milicua JCG, Gomez R, Macarulla JM & Britton G (1986) Purification and characterization of the blue carotenoprotein from the carapace of the crayfish *Procambarus clarkii* (Girard). *Biochim Biophys Acta* **881**, 446–455.
27 Terada S, Fujimura S, Kino S & Kimoto E (1994) Purification and characterization of three proteinase inhibitors from Canavalia lineata seeds. *Biosci Biotechnol Biochem* **58**, 371–375.
28 Gittleman J & Harvey PH (1980) Why are distasteful prey not cryptic? *Nature* **286**, 149–150.
29 Snyder NFR & Snyder HA (1971) Defenses of the Florida apple snail *Pomacea paludosa*. *Behaviour* **40**, 175–215.
30 Randall D, Burggren W & French K (1997) Energy acquisition: feeding, digestion and metabolism. In *Eckert Animal Physiology. Mechanisms and Adaptations* (Randall D, Burggren W & French K, eds), pp. 683–724. Freeman, New York, NY.
31 Denbow DM (2000) Gastrointestinal anatomy and physiology. In *Sturkie's Avian Physiology* (Whittow GC, ed), pp. 299–325. Academic Press, Boston, MA.
32 Heras H, Garín CF & Pollero RJ (1998) Biochemical composition and energy sources during embryo development and in early juveniles of the snail *Pomacea canaliculata* (Mollusca: Gastropoda). *J Exp Zool* **280**, 375–383.
33 Bradford MM (1976) A rapid and sensitive method for the quantitation of microgram quantities of protein utilizing the principle of protein-dye binding. *Anal Biochem* **72**, 248–274.
34 Davis B (1964) Disc electrophoresis. II. Method and application to human serum proteins. *Ann N Y Acad Sci* **121**, 404–428.
35 Margolis J & Wrigley CW (1975) Improvement of pore gradient electrophoresis by increasing the degree of cross-linking at high acrylamide concentration. *J Chromatogr* **105**, 204–209.
36 Svergun DI (1999) Restoring low resolution structure of biological macromolecules from solution scattering using simulated annealing. *Biophys J* **76**, 2879–2886.
37 Volkov VV & Svergun DI (2003) Uniqueness of ab initio shape determination in small-angle scattering. *J Appl Crystallogr* **36**, 860–864.
38 Deutscher MP (1990) Section II. General methods for handling proteins and enzymes. In *Guide to Protein Purification. Methods in Enzymology* (Deutscher MP, ed), pp. 19–92. Academic Press, New York, NY.
39 Moreno FJ, Maldonado BM, Wellner N & Mills EN (2005) Thermostability and in vitro digestibility of a purified major allergen 2S albumin (Ses i 1) from white sesame seeds (*Sesamum indicum* L.). *Biochim Biophys Acta* **1752**, 142–153.
40 Andrade MA, Chacón P, Merelo JJ & Morán F (1993) Evaluation of secondary structure of proteins from UV circular dichroism using an unsupervised learning neural network. *Prot Eng* **6**, 383–390.
41 Villarroel A, Garate AM, Gomez R & Milicua JCG (1985) A blue carotenoprotein from *Upogebia pusilla*. Purification, characterization and properties. *Comp Biochem Physiol* **81**, 547–550.
42 Chayen NE, Cianci M, Grossmann JG, Habash J, Helliwell JR, Nneji GA, Raftery J, Rizkallah PJ & Zagalsky PF (2003) Unravelling the structural chemistry of the colouration mechanism in lobster shell. *Acta Crystallogr* **59**, 2072–2082.
43 Armitt GM (1981) *Studies on invertebrate carotenoproteins*. PhD Thesis, University of Liverpool, Liverpool, UK.
44 Salares VR, Young NM, Bernstein HJ & Carey PR (1979) Mechanisms of spectral shifts in lobster carotenoproteins. The resonance raman spectra of ovoverdin and the crustacyanins. *Biochim Biophys Acta* **576**, 176–191.